# Synthesis of high surface area activated carbon from eucalyptus bark for the removal of methylene blue

Shailesh Kumar Yadav[a], Kiran Mahadeo Subhedar[a], Sanjay Ranganth Dhakate[a] & Bhanu Pratap Singh[a, b*]

[a]Advanced Carbon Products and Metrology, Advanced Materials and Devices Metrology
CSIR-National Physical Laboratory, Dr. K.S. Krishnan Marg, New Delhi-110 012, India
[b]Academy of Scientific and Innovative Research (AcSIR), Ghaziabad, Uttar Pradesh 201 002, India

In present study, high surface area ($1852 m^2 g^{-1}$) activated carbon was synthesized by single step thermo chemical activation of agro-waste lignocellulose biomass (eucalyptus bark).The synthesized activated carbon has been characterized using scanning electron microscopy, energy-dispersive-X-ray spectroscopy and BET surface area analyser. The eucalyptus bark derived activated carbon (EBAC) was used to remove methylene blue (MB) from waste water. The pH, contact time and concentration of dye were optimized and it was found that at pH of 5.5-6.5 at the room temperature, maximum removal of dye was observed. The obtained time data follows the pseudo second order kinetics. The effect of concentration study was carried out with varying concentration at optimized pH and time. The maximum adsorption capacity is obtained to be 7.15 mg/g. To understand the adsorption process, the Dubinin–Radushkevich (D–R) isotherm and Freundlich isotherm were used for fitting of equilibrium data. The fitted data follows D-R isotherm which reveals the physisorption process during adsorption of dye.

Keywords: Activated carbon, Methylene blue, Adsorption, Isotherm, Kinetics

## 1 Introduction

Activated carbon is a porous carbonaceous material with the highly developed surface area and rich surface groups are widely used in numerous applications, including adsorption, catalyst support, gas separation and storage, solvent recovery and decolorizing, super capacitors, removal of pollutants by adsorption from liquid or gas phase and as electrodes[1]. Furthermore, newer applications are ever emerging, particularly those concerning environmental protection and technological development.

The internal porosity and their related properties such as surface area, pore volume, pore size distribution, and the presence of functional groups on pore surfaces play a significant role in the adsorptive capacities of activated carbons (ACs)[2]. Activated carbons with abundance of microspores are extensively used for adsorption of small molecule pollutants, and highly developed mesoporous activated carbons are used for the adsorption of larger molecules such as dyes[3]. The factors such as the nature of raw materials, the activation method, the activating agent and the conditions of activation process affect the textural and chemical characteristics of the activated carbons. In recent years, activated carbon is being produced from a large number of easily available and low-cost materials such as agricultural products like paulownia wood[4], vine shoots[5], fire wood[6], marigold straw[7], candlenut shell[8], corncob[9], coconut shells[10], reedy grass leaves[11], lotus stalks[12], and buriti shells[13]. The choice of the starting material for the preparation of ACs depends on availability, cost and purity; the manufacturing process and intended application of the product are important considerations as well. The precursors used for the production of ACs are materials rich in carbon, such as coal, lignite and wood, among others. Although coal is a commonly used precursor, agricultural waste of specific types is a better choice.

Agricultural wastes are considered to be very important feedstock, since they are renewable sources and low cost materials[4]. In pulp and paper industry, eucalyptus bark is generated as one of the by-products from the raw material preparation section. This bark contained a reasonably high content of carbon and could also be used as a raw material for synthesis of ACs. In this study, eucalyptus bark was utilized as a raw material for the production of activated carbon powder. It is a starting material with an interesting potential owing to its granular shape and its ready

___

*Corresponding author
(E-mail: bps@nplindia.org, bpsingh2k4@yahoo.com)

availability in various countries. Activated carbon is among the potential conversions, with applications in the removal of dyes, odors, tastes, and contaminants, in water purification and other decontamination processes[14]. Eucalyptus bark is a lignocellulose material, with hemicellulose, cellulose and lignin as the main components. Eucalyptus bark can be a very adequate feedstock. Therefore, in this study, Eucalyptus bark has been used to synthesize AC and it has been explored for methylene blue (MB) removal form waste water.

## 2 Material and Methods
### 2.1 Preparation of activated carbon
Eucalyptus bark, collected from plantation area in CSIR-National Physical Laboratory, New Delhi, India, was used as a precursor. The eucalyptus bark was washed with distilled water and then oven dried overnight at 65 °C. The bark was crushed, transformed into powder and sieved through the 50mesh. The sample (15 gm, eucalyptus bark powder) was impregnated into 60 ml phosphoric acid solution (98% by weight, impregnation ratio of 1:4). Then this mixture was stirred at room temperature for 20 hours. After mixing, carbonization of acid-impregnated eucalyptus bark was carried out in a quartz boat and it was kept in the stainless steel reactor provided with gas inlet and outlet. This was placed in a horizontal tubular furnace. It was heated from room temperature to 550 °C (i.e carbonization temperature) in inert atmosphere of nitrogen (flow rate 2 ml/min).The heating rate was 5 °C/min with holding time of 30 min.After heating, the system was allowed to naturally cool down to room temperature under the same flow of nitrogen gas and product obtained was washed with hot water till pH 7 was reached and finally obtained material was dried overnight in oven at temperature 105 °C.

### 2.2 Characterization
The surface area of eucalyptus bark derived activated carbon (EBAC) was examined by the nitrogen adsorption–desorption isotherm measured using the surface area analyzer (Quantachrome Autosorbi Q). Further, pore volume, pore size distribution were also studied. The Brunauer-Emmett-Teller equation was used for estimating the surface area of EBAC. Moisture, volatile matter and ash content of eucalyptus bark were determined by thermo gravimetric analysis (TGA) at temperatures of 1000 °C, using a METTLER TOLEDO make TGA. A ramp of temperature of 10 ºC/min was used. Moisture and volatile content were measured under continuous Air flow of 100 ml/min, where as equivalent air flow was used for ash content determination. Scanning electron microscopy (SEM) was performed to study the morphology of the EBAC.

### 2.3 Adsorptive removal of organic dyes
The organic MB dye used for adsorptive removal by EBAC adsorbent and its structure and relevant data are provided in Table 1.
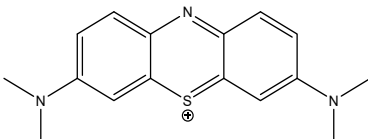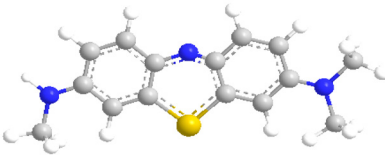
The batch-mode adsorptions experiments were performed to understand the adsorption characteristics, capacity, and efficiency of EBAC adsorbent. The batch adsorption experiments were conducted in a set of 500 ml of flask containing adsorbent and 20 ml of MB solution with various initial concentrations. After decantation and filtration, the equilibrium concentrations of dye in the solution were measured at 664 nm using UV-visible spectrophotometer. The pH of solution was adjusted with 1N HCl and 1N NaOH solutions. The amount of dye adsorbed and percentage removal of MB were calculated using Equation (1) and (2), respectively:

$$q_e = \frac{c_i - c_f}{c_i} * \frac{V}{M} \qquad \qquad \dots (1)$$

$$\% \text{ Removal of MB} = \frac{C_i - C_f}{C_i} * 100 \qquad \dots (2)$$

In these equations, $q_e$ is amount of dye in mg per gram of adsorbent. $C_i$ and $C_f$ are initial concentration and equilibrium concentration of MB (mg/L), respectively. V (L) is volume of solution and M is mass of adsorbent in gram.

Table 1 — MB dye used for adsorptive removal by EBAC adsorbent.

| Name and structure of organic dye | Structural model | Molecular weight | Estimate diameter(Å) |
|---|---|---|---|
| Methylene blue(MB) | | 319.8 | 13.95 |

# 3 Results and Discussion

## 3.1 Characterization of adsorbent material

### 3.1.1 Morphological analysis and determination of textural properties

SEM images of EBAC with 1:4 impregnation ratio at activation temperature of 550 ºC are shown in Fig. 1. SEM images illustrated irregular structure with cracks and crevices on the surface of the AC. This confirmed amorphous and heterogeneous structures.

The qualitative composition given by EDS is shown in Fig.1 reveals that particles contain predominantly carbon, as well as oxygen and phosphorous.

### 3.1.2 BET and pore size distribution

Textural features of EBAC were estimated by nitrogen adsorption-desorption isothermal analysis. The nitrogen sorption isotherm shown in Fig. 2a follows the type IV isothermal having H4 type hysteresis loop, which suggests the presence of irregularly shaped mesopores. The BET surface area of EBAC based on nitrogen sorption isotherm was estimated to be 1852 $m^2$/g. The average pore diameter for EBAC was found to be 4.15nm based on the BJH model.

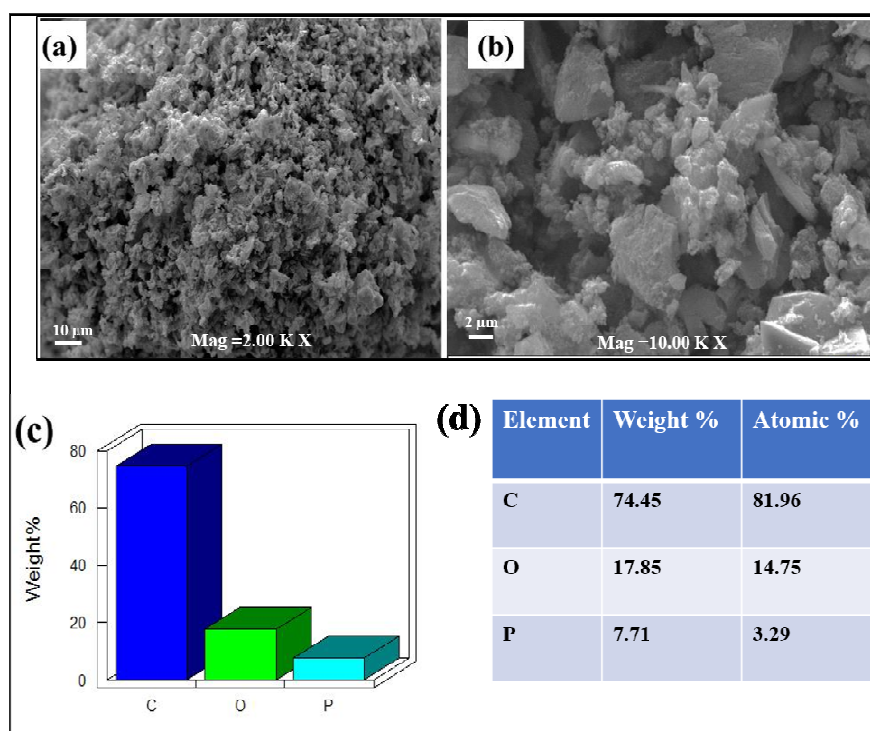The low average pore size was further supported by a major fraction of mesoporisty as shown in the



| Element | Weight % | Atomic % |
|---------|----------|----------|
| C | 74.45 | 81.96 |
| O | 17.85 | 14.75 |
| P | 7.71 | 3.29 |

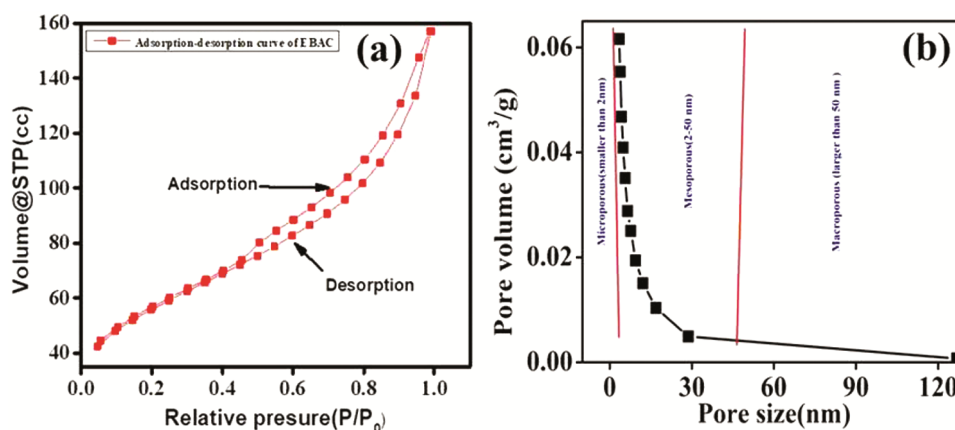Fig. 1 — SEM Image of EBAC at 10µm and 2 µm magnification and EDS spectrum of EBAC.



Fig. 2 — (a) Nitrogen adsorption–desorption isotherm for EBAC at −196 °C and (b) Pore size distribution of EBAC.

Fig. 2b. The activated carbon (EBAC) prepared at 550 °C exhibited the highest surface area and lowest pore diameter which is essential for fast diffusion/transport of pollutants through the micro and mesopores channels. They also furnished significantly high and accessible surface area for efficient adsorption of organic pollutants[15].

### 3.1.3 Thermo gravimetric analysis (TGA)

Figure 3 shows the results from TGA analysis carried out on EBAC and the decomposition of EBAC. The de-volatilization process is sequential and depends on the temperature of the material (see Fig.3). The first stage is comprised between 20-120 °C and corresponds to water evaporation from the biomass, and subsequently between 120-300 °C is a region with no appreciable biomass weight loss, where in small quantities of some light gases are released such as CO,
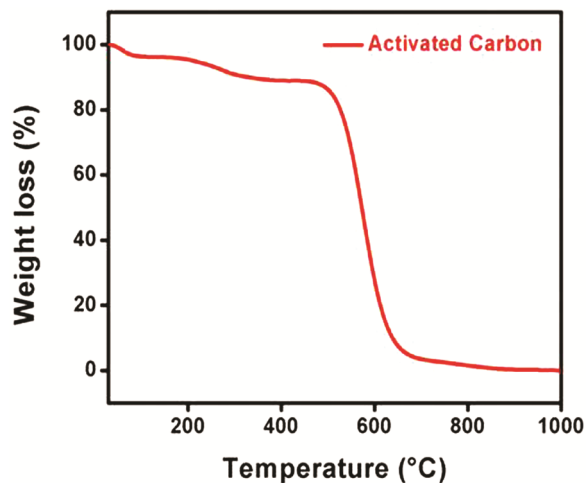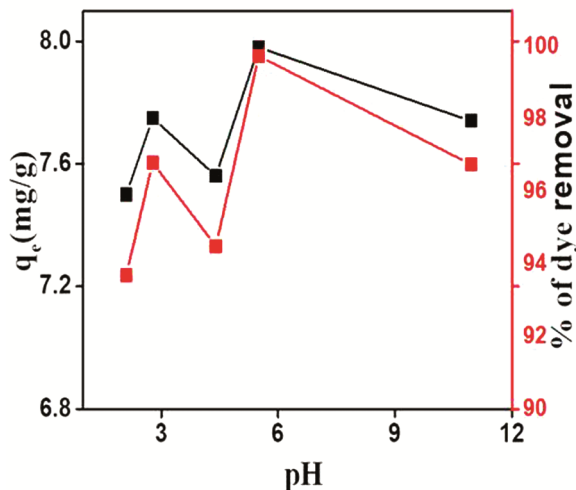


Fig. 3 — Thermogram of EBAC.



Fig. 4 — Effect of solution pH on the adsorption of MB ($C_0$ = 8 ppm, w = 1 g/L, T = 300 K).

$CO_2$ and steam, coming mainly from dehydration reactions, de-carboxylation from R-OH groups belonging to hemi-cellulose and lignin[16]. For cellulose, it has been demonstrated[17] that between 200-350°C, the de-polymerization reactions gives rise to oligomers and anhydrous sugars known by many researchers as "active cellulose" and "molten cellulose" or simply "intermediary liquid compound"[18].

The highest weight loss occurred in between 500 and 600 °C (about 90%), corresponding to the maximum rate of volatiles released. In this stage, random fragmentation of cellulose, hemicelluloses, and glycosidic bonds generates volatile compounds with high oxygen content, leaving a carbonaceous residue known as char.

### 4 Batch-mode adsorptive removal of organic dyes methylene blue

#### 4.1 Effect of pH

The pH of a dye solution is important influencing factors affecting the dye structure and adsorption surface, ionization degree and removal efficiency. In present study, the effect of the pH was studied at different pH values Fig. 4

Figure 4 shows the effect of pH on adsorption onto EBAC. The maximum MB removal was observed at pH 5.5. It is because the basic dye gives positively charged ion when dissolved in water. Thus in acidic medium positively charged surface of sorbent tends to oppose the adsorption of the cationic adsorbate. When pH of the dye solution increased, the surface acquires a negative charge, there by resulting in an increased adsorption of MB due to an increase in the electrostatic attraction between positively charge dye and negatively charge adsorbent[19].

#### 4.2 Kinetics study

Kinetics study reveals the sorption behaviour of adsorbent forward adsorbate at equilibrium time (t). The removal of MB by EBAC as a function of time is shown in Fig. 5.

In order to have better understanding of the adsorption process, two adsorption kinetic models the pseudo-first order and pseudo second order kinetics model applied for the fitting of data.

The formula of pseudo first order rate expression is given as:

$$\log(q_e - q_t) = log q_e - \frac{k_1}{2.303} \qquad \ldots (3)$$

where, $q_e$ and $q_t$ are the amount of dye adsorbed on sorbent at equilibrium and time t (mg/g) and $k_1$ is the pseudo first order rate constant (min$^{-1}$). A plot of log
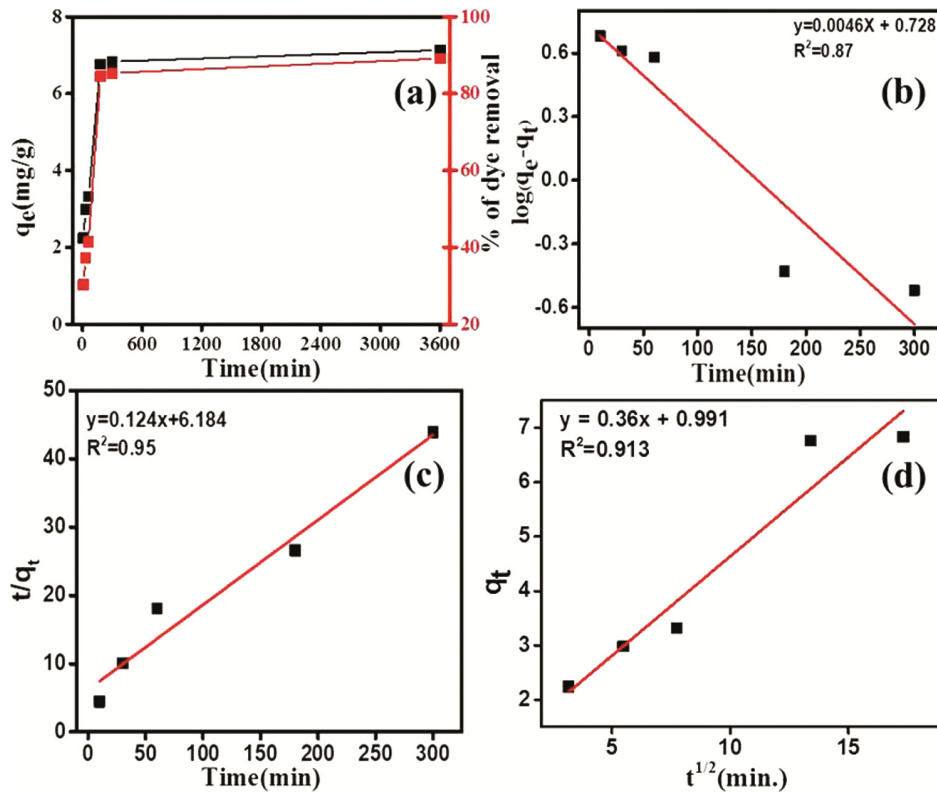
Fig. 5 — (a) Effect of contact time on MB removal (b) Pseudo first order kinetic plot for MB adsorption (c) Pseudo second order kinetic plot for MB adsorption and (d) Intra-particle diffusion model fitting curve.

($q_e$-$q_t$) versus t gives a linear relationship, from which the value of $k_1$ and $q_e$ can be determined from the slope and intercept. The linearized form of pseudo second order rate expression is given as[20]:

$$dq_1/dt = K_2(q_e - q_t)^2 \qquad \dots (4)$$

$$\frac{t}{q_t} = \frac{1}{k_2 \, q_e^2} + \frac{t}{q_e} \qquad \dots (5)$$

where $q_e$ is the amount of adsorbate adsorbed per unit mass of sorbent at equilibrium (mg/g), $q_t$ is the amount of adsorbate adsorbed at contact time t (mg/g) and $k_2$ is the pseudo second order rate constant (g/mg min). A plot of $t/q_t$ versus t gives a linear relationship, from which $q_e$ and $k_2$ can be determined from the slope and intercept[21].

The data for the adsorption of MB on EBAC were fitted with pseudo first and pseudo second order kinetic models and the results are presented in Table 2. The correlation coefficient of determination $R^2$ was found to be approximate for pseudo second order kinetic model (0.95) is greater than for pseudo first order kinetic model (0.87) (Table 2, Fig. 5).

Table 2 — Kinetics parameters for the sorption of MB onto activated carbon.

| Pseudo first order model | $q_e$ (mg/g) 5.34 | $R^2$ |
| $k_1$ (min$^{-1}$) 0.010 | | 0.87 |
| Pseudo second order model | $q_e$ (mg/g) 8.06 | $R^2$ |
| | | 0.95 |
| $k_2$ g/(mg-min)0.0024 | | |
| Intraparticle diffusion model | C (mg/g) 0.99 | $R^2$ |
| | | 0.91 |
| $K_d$ (mg/g min) 0.36 | | |

This follows the pseudo second order kinetics and the rate of adsorption process is fast depending on the concentration of adsorbate and adsorbent.

The intraparticle diffusion equation is expressed as follows:

$$qt = k_{id} \, t^{\frac{1}{2}} + C \qquad \dots (6)$$

where, $k_{id}$ is the intra particle diffusion rate constant (mg/ g min$^{1/2}$). The data for intra particle diffusion are given in Table 2. The linear portion of the plot does not pass-through origin. This deviation from the origin may be due to the variation of mass transfer in the initial and final stages of the adsorption process. This confirms that the adsorption of MB on

EBAC was a multi-step process involving adsorption on the external surface and diffusion into the interior[22]. The effect of contact time on the removal of MB is shown in Fig. 5(a). It showed that 90% dye removal takes place in 3 hours for EBAC. The equilibrium was reached after 5 hours. The change in the rate of adsorption might be due to fact that initially all the adsorbent sites are vacant and solute concentration gradient was very high. Later, the lower adsorption rate is due to a decrease in number of vacant sites of adsorbent and dye concentrations. The decreased adsorption rate, particularly, toward the end of experiments, indicates the possible monolayer formation of MB on the adsorbent surface[19]. This may be attributed to the lack of available active sites required for further uptake after attaining the equilibrium[23].

### 4.3 Adsorption isotherm

Adsorption isotherm describes the equilibrium relationship between solid and liquid interface and can be explained on the basis of Langmuir, Freundlich, Tempkin, and Dubinin-Radashkevich (D-R) isotherm. In the proposed study, we used only D–R isotherm model and Freundlich isotherm. The D-R isotherm describes the experimental data better than Freundlich model. The correlation coefficient $R^2$ of D-R model, which is found to be 0.93(Table 3), is higher the Freundlich 0.74.

The Dubinin–Radushkevich (D–R) isotherm model, which is based on the Polanyi theorem, can provide information about the energy required for the adsorption process and mechanism involved. The D–R isotherm assumes a Gaussian (normal) distribution of energy sites[24]. Thenon-linear and linearized forms of the equation are:

$$q_e = q_s \exp\left(-K_{DR} \in^2\right) \qquad \text{... (7)}$$

$$ln q_e = ln q_s - K_{DR} \in^2 \qquad \text{... (8)}$$

where, $q_s$ (mg/g) is the adsorption capacity and $K_{DR}$ is a constant related to adsorption energy. A plot of $ln q_e$ vs. $\in^2$ based on the linear D–R equation should give a straight line from which $K_{DR}$ and $q_s$ can be determined from the slope and intercept, respectively.

where, $\varepsilon$ is the polanyi potential $(ln(1 + \frac{1}{c_e})$, and R, T, $q_e$ and $C_e$ are the gas constant (8.314 J/mol K),

temperature in Kelvin, amount of dye in mg/gram of adsorbent and equilibrium concentration in solution, respectively. The mean free energy of adsorption ($\in$) for the MB-EBAC using Eq. 8, the magnitude of which may provide useful information with regards to the adsorption mechanism, whether it is a chemical or physical process[25].

$$\in = \frac{1}{\sqrt{2K_{DR}}} \qquad \text{... (9)}$$

The values of $q_s$ and $K_{DR}$ obtained from the linear plot of the D–R equation as well as the mean free energy of adsorption ($\in$ = 1.31 kJ/mol(Table 3))were determined from Eq. 8. The value of free energy was obtained in the range 8-16 kJ/mol and signifies ion-exchange mechanism or chemisorptions during the adsorption process. It is generally observed that, value of $\in<$8kJ/mol represents the physical adsorption because of the electrostatics interaction between the opposite charge present in the adsorbate and adsorbent. In the present study, the free energy value suggests that MB adsorption on EBAC is physisorption.

Effect of adsorbent dose and initial dye concentration, the adsorbent doses varied from 5mg - 35mg/20 ml. It is evident from Fig. 6(b) that the MB removal increased sharply with an increase in the adsorbent concentration from 1ppm to 20ppm. This is due to the availability of more adsorbent sites as well as greater availability of specific surfaces of the adsorbents as shown in Fig. 6(a). However, no significant changes in removal efficiency were observed beyond 30mg adsorbent dose. Due to agglomeration of adsorbent particles, there was no increase in effective surface area of EBAC. So, 30mg was considered the optimal dose for EBAC loading[19].

The effect of dye concentration on the sorption of MB onto EBAC was carried out in the concentration range of 1 ppm to 20 ppm (Fig. 6a). Equilibrium adsorption capacity increased with an increase in MB concentration from 1ppm to 20ppm. Further increase in dye concentration showed no significant change in removal efficiency. This is due to the fact that with increased dye concentration, the driving force for mass transfer also increases. At low concentrations,

Table 3 — Result of isotherm plots for the adsorption of MB onto EBAC

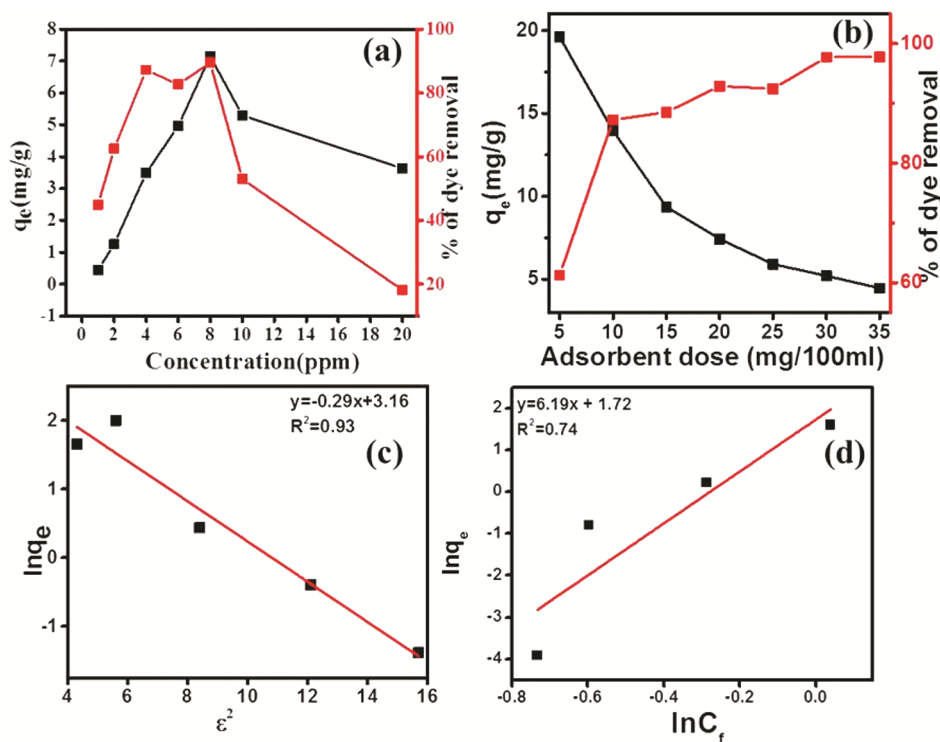| Model | Isotherm constant | | | |
|---|---|---|---|---|
| The Dubinin–Radushkevich (D–R) isotherm | $q_s$ (mg /g) 13.95 | $K_{DR}$(L/mg) 0.29 | Energy(E)(kj/mol) 1.31 | $R^2$ 0.93 |

Fig. 6 — (a) Effect of initial dye concentration on EBAC($C_0$ = 2 - 20 ppm, w = 1 g/L, T = 300 K), (b) Effect of adsorbent dose on MB removal ($C_0$ = 8 ppm, w = 1 g/L, T = 300 K), (c) The Dubinin–Radushkevich (D–R) isotherm model and (d) Freundlich adsorption isotherm.
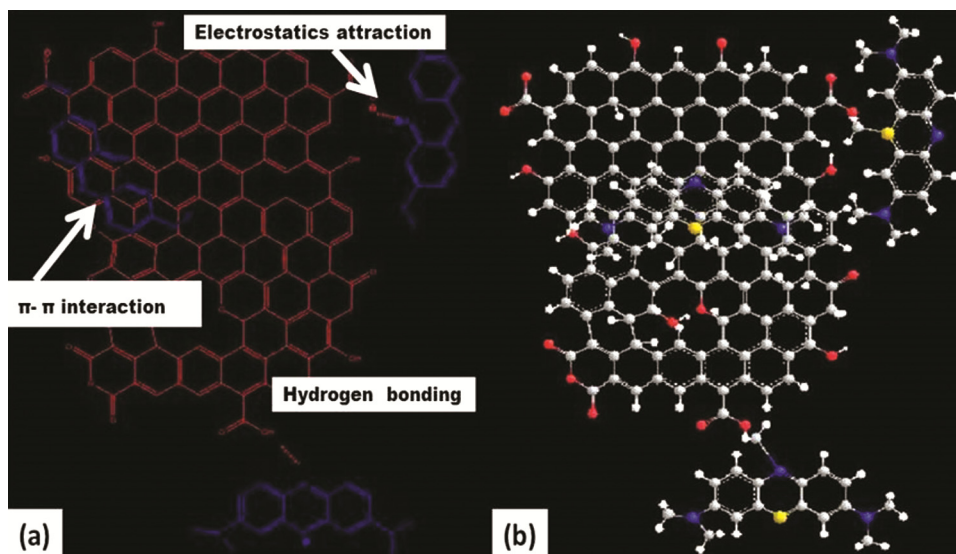


Fig. 7 — Representative structural model of EBAC along with possible interaction pathways with MB.

there will be unoccupied active sites on the adsorbent surface. Above optimal MB concentration, there is lack of active sites required for the adsorption of dye[26]. This retards the overall MB adsorption by activated carbon. The mechanism for the removal of MB by using EBAC is shown in Fig. 7. As, it is already established in this study that MB has been removed by physio-sorption mechanism, so mainly two types of interaction took place, i.e electrostatic and π-π interaction.

**5 Conclusions**

In this study, eucalyptus bark derived activated carbon (EBAC) showed promising adsorption capacity for methylene blue (MB) removal. The operating parameters for the maximum sorption were dye

solution concentration of 8 ppm, sorbent dose of 30mg/20 ml, contact time of 180 min and temperature of 303K. Removal of MB dye is pH dependent and the maximum removal was attained at pH 5.5. Equilibrium data were fitted well in the D-R isotherm model which confirmed that sorption occurred through physical interaction. The kinetics of adsorption process was found to follow the pseudo second order kinetic model. The second order model was applied to study the mechanism of adsorption and calculated $q_e$ value agreed well with the experimental values. In conclusion, EBAC can be used as an effective adsorbent for the removal of methylene blue from waste water.

## Acknowledgement

## References
1 Yu M, Li J & Wang L,*Chem Eng J,* 310 (2017) 300.
2 Miguel G S, Fowler G D, Dall'Orso M & Sollars C J, *J Chem Technol Biotechnol*, 77 (1) (2002) .
3 Tamai H, Yoshida T, Sasaki M & Yasuda H, *Carbon*, 37 (6) (1999) 983.
4 Yorgun S, Yıldız D, *J Taiwan Inst Chem Eng*, 53 (2015) 122.
5 Corcho-Corral B, Olivares-Marín M, Fernández-González C, Gómez-Serrano V & Macías-García A, *Appl Surf Sci*, 252 (17) (2006) 5961.
6 Danish M, Hashim R, Ibrahim M M & Sulaiman O, *Wood Sci Technol*, 48 (5) (2014) 1069.
7 Qin C, Chen Y & Gao J-M, *Mater Lett*, 135 (2014) 123.
8 Turmuzi M, Daud W R W, Tasirin S M, Takriff M S & Iyuke S, *Carbon*, 42 (2) (2004) 453.
9 Sych N, Trofymenko S, Poddubnaya O, Tsyba M, Sapsay V, Klymchuk D & Puziy A, *Appl Surf Sci,* 261 (2012) 75.
10 Azevedo D C, Araujo J C S, Bastos-Neto M, Torres A E B, Jaguaribe E F & Cavalcante C L, *Microporous Mesoporous Mater*, 100 (1-3) (2007) 361.
11 Xu J, Chen L, Qu H, Jiao Y, Xie J & Xing G, *Appl Surf Sci*, 320 (2014) 674.
12 LiuH, Wang X, Zhai G, Zhang J, Zhang C, Bao N & Cheng C, *Chem Eng J*, 209 (2012) 155.
13 PezotiJr O, Cazetta A L, Souza I P, Bedin K C, Martins A C, Silva T L & Almeida V C, *J Ind Eng Chem*, 20 (6) (2014) 4401.
14 Yakout S & El-Deen G S, *Arab J Chem*, 9 (2016) S1155.
15 Gupta K & Khatri O P, *Chem Eng J*, 378 (2019) 122218.
16 Saldarriaga J F, Aguado R, Pablos A, Amutio M, Olazar M, Bilbao J, *Fuel*, 140 (2015) 744.
17 Chatterjee P K & Conrad CM, *J Polym Sci, Part A: Polym Chem*, 6 (12) (1968) 3217.
18 LédéJ, *J Anal Appl Pyrolysis*, 94 (2012) 17.
19 Pathania D, Sharma S & Singh P, *Arab J Chem*, 10 (2017) S1445.
20 Hamdaoui O & Chiha M, *Acta Chim Slov*, 54 (2007) (2) 407.
21 Bhattacharyya K G & Sharma A, *Dyes pigm*, 65 (1) (2005) 51.
22 Kumar K V & Kumaran A, Biochem. Eng. J. 27 (1) (2005) 83.
23 Shakoor S & Nasar A,*Groundwater for Sustainable Development, 5 Elsevier,* (2017) 152.
24 Hutson N D & Yang R T, *Adsorption*, 3 (3) (1997) 189.
25 Erdogan F O, *Int J Chem React Eng*, 17(2019) (5) 20180134.
26 de Farias Silva C E, da Gama B M V, da Silva Gonçalves A H, Medeiros J A& de Souza Abud A K, *J King Saud Univ Eng Sci*, (2019) 351.